Tellus (2005), 57A, 290–307
Printed in UK. All rights reserved

TELLUS

Winter climate regimes over the North Atlantic and European region in ERA40 reanalysis and DEMETER seasonal hindcasts

By C. FIL* and L. DUBUS *Electricité de France, Research and Development Division, SPE 6 quai Watier, 78 400 Chatou, France*

(Manuscript received 30 March 2004; in final form 29 November 2004)

ABSTRACT

The observed and simulated low-frequency winter variability of the North Atlantic and European region is investigated based on the climate regimes paradigm. Empirical orthogonal functions and cluster analyses are used to describe the variability of monthly mean sea level pressure over the 1958–2001 period, both in the European Centre for Medium-Range Weather Forecasts (ECMWF) 40-yr reanalysis (ERA40) data set and the multi-model ensemble hindcasts from the DEMETER seasonal forecasting system.

The clustering partition of ERA40 fields yields four climate regimes. The first two clusters capture the negative and positive phases of the North Atlantic Oscillation (NAO), respectively. The third and fourth clusters, respectively, display a strong anticyclonic ridge off western Europe almost covering the entire basin and a zonal pressure dipole between Greenland and Scandinavia, with a clear south-eastward extension of the low-pressure anomalies towards the Iberian peninsula.

DEMETER seasonal forecasting models are able to reproduce the multimodal variability of the winter atmosphere with the same number of modes. For the ECMWF model, the pressure patterns of the regimes are very similar to those obtained for ERA40. For the six other models, the two NAO modes are well reproduced but the two other regimes are more different. In terms of forecasts, different scoring methods are used to evaluate the ability of the models to predict the correct regimes for a given date, but scores appear to be quite low.

Then, the link between the pressure regimes and the corresponding temperature fields is investigated using different composite methods. All the ERA40 regimes are characterized by specific patterns of temperature. DEMETER models are also able to reproduce the temperature impacts of the different regimes. Thus, some predictability could arise from reliable seasonal predictions. Indeed, if models are able to forecast pressure fields at a monthly time-scale, it should allow us to forecast which regime will be excited and then to deduce the corresponding large-scale pattern of temperature anomalies.

1. Introduction

The European energy sector is highly dependent on climate conditions. In winter, for example, a negative temperature anomaly of 1° over France implies an overconsumption of around 1200 MW, due to the importance of electrical heating. On the other hand, a positive anomaly of 1° in summer implies an increase in consumption for air conditioning of 200 MW, which can be even more important in the case of a long and high-amplitude heat wave, as in the summer of 2003. Heat waves in summer also have impacts on production capacities. National regulations exist that fix the temperature of water rejected by power plants, which must not overcome some thresholds. Thus, heat waves can increase the river temperatures, implying less flexibility for power plants cooling. In the case of a very cold wave in winter, cooling of power units could be perturbed by ice formation at the water intake. Of course, precipitations, snow melting and river flows also play an important role: they control the hydraulic power production capacity, and the availability of cooling for power production units. In this field again, there are strict regulations, concerning the minimum level of water downstream of the plants ('touristic level'), or the minimal flows to ensure agricultural irrigation, for example. Climate conditions also explain an important part of electricity market prices all over Europe.

For all these reasons, Electricité de France (EDF) has been driving research on weather and climate predictions for many years. As electricity cannot be stocked, there is a permanent need to ensure the balance between electricity demand and

*Corresponding author.
e-mail: clarisse.fil@edf.fr

offer. On the medium range (up to 8–10 d), operational weather predictions are quite good and allow an efficient management of production. On longer time-scales, seasonal climate forecasts have rapidly improved in the last years, and could present some interests for EDF. The Research and Development Division is involved in research projects, in order to evaluate the potential value of seasonal forecasts over Europe and other parts of the world for EDF activities.

This paper is about winter climate regimes in the North Atlantic/European sector, as observed in the European Centre for Medium-Range Weather Forecasts (ECMWF) 40-yr reanalysis (ERA40; Simmons and Gibson, 2000) and simulated by the DEMETER seasonal forecasts system (Palmer et al., 2004). The work focuses on winter because atmospheric variability is higher in winter than in other seasons, but the method was also applied to other seasons.

Local climate in Europe is influenced by large-scale atmospheric circulation (particularly over the North Atlantic and European region) and by oceanic conditions (essentially from the North Atlantic). The European weather, particularly in winter, is often characterized by strong eastward air flow between the 'Icelandic low' and the 'Azores high', and by a 'storm track' of weather systems, which moves towards Europe (Rodwell et al., 1999). The North Atlantic Oscillation (NAO) is an important mode of variability in this region that is characterized by some intensity changes of the Icelandic low and Azores high, which are related to the position and intensity of the storm track and influence the local temperature and precipitations in Europe (Hurrell, 1995; Hurrell et al., 2003). The storm track and westerlies are sometimes perturbed by the presence of blocking highs (Sanders, 1953) that explain some cold waves in winter and severe droughts in summer (Vautard, 1990). The European climate and the NAO are also influenced by the Atlantic oceanic conditions (Rodwell et al. 1999; Cassou et al., 2004a; Cassou et al., 2004b) and by some other regions, such as the tropical Pacific, via the teleconnections between the El Niño Southern Oscillation (ENSO) phenomenon and the temperature in some parts of Europe (Halpert and Ropelewski, 1992).

All these phenomena are interesting to understand in order to explain local climate in Europe. This is the reason why there have been different studies in the past few decades to characterize the natural climate variability over the North Atlantic and European (NAE) region on monthly to decadal time-scales. To determine if atmospheric variability is multimodal at these time-scales, some linear techniques have been traditionally used. For instance, the empirical orthogonal functions (EOFs) that derive from monthly meteorological fields are some modes of atmospheric variability. To obtain more physically meaningful and statistically stable patterns, a non-linear perspective is adopted and the atmospheric variability is here investigated based on the climate regimes paradigm. Weather and climate regimes (Lorenz 1963) are defined as attractors that correspond to peaks in the probability density function of the climate phase space; they are characterized by recurrence, quasi-stationarity and persistence (Michelangeli et al., 1995). The difference between climate and weather regimes is the time-scale: climate regimes provide from analysis performed on monthly (or seasonal) fields while weather regimes (Vautard, 1990; Michelangeli et al., 1995) come from analysis of daily fields. This study is mainly based on cluster analysis. This is a non-linear statistical technique that permits us to gather elements in small specific groups, which are defined as the climate regimes.

The idea is to characterize the atmospheric variability of the NAE region using the ERA40 reanalysis data set in order to compare the natural variability to that simulated by the DEMETER models. To this purpose, after a brief EOF study, we investigate the climate regimes of the NAE region defined by the cluster analysis of monthly pressure fields in winter (as in Cassou et al., 2004a) and determine the influence of these regimes on local temperature and precipitations in Europe and in the NAE region. In a second step, the same processes are applied to seasonal forecasting models from the DEMETER system. The ability of the models to reproduce the observed variability is investigated by comparing the pressure regimes and the temperature impacts of the models with ERA40 regimes and impacts. The quality of the forecasts is studied in terms of regime prediction, as some predictability could arise from successful forecast of the type of regime and the ability to deduce some impacts on temperature, for instance.

The paper is organized as follows. In Section 2, data and methods are described. In Section 3, cluster analysis is applied on the ERA40 data set in order to describe observed variability. The same analysis is then applied to seasonal simulations of the DEMETER system to determine if dynamical models correctly simulate winter atmospheric variability; results are presented in Section 4. Regime impacts are studied in Section 5; analysis is performed on both observed and simulated regimes. Section 6 contains a summary and a brief discussion.

2. Data and methods

The observed winter atmospheric variability is described using the ECMWF ERA40 over the 1958–2001 period and the National Center for Environmental Prediction (NCEP) reanalysis over the 1948–2003 period. The analysis is performed on monthly mean sea level pressure (MSLP) and geopotential height at 500 hPa (Z500) fields, which describe large-scale airmass movements. Winter corresponds to December, January and February (DJF). The analysis is made on anomaly fields, calculated with respect to monthly climatologies. Data resolution is 2.5° in latitude and longitude. Data are available over the whole globe, so EOF and cluster analysis are performed on different NAE regions comprised between 100°W and 80°E and in the Northern Hemisphere. As similar results are obtained and most of the variance of this zone is located in the North Atlantic region (especially around Iceland), we have chosen to present only the results of the

analysis on the (80°W–30°E/20°N–80°N) domain, which is an area that influences climate in western Europe (as in Cassou et al., 2004a). For temperature impacts, 2-m temperature (T2m) and 850-hPa temperature (T850) are considered over the (90°W–60°E, 15°N–90°N) region. This area is larger than that used for the cluster analysis itself in order to have a larger vision of impacts over Europe. T850 is close to the surface sensible temperature but its variability is less dispersed so that patterns show less small-scale features.

Dynamical prediction of atmospheric variability is investigated in the DEMETER prediction system (Palmer et al., 2004). The DEMETER (Development of a European Multi-model Ensemble system for seasonal to inTERannual prediction) project was conceived, and funded under the European Union Vth Framework Environment Programme. The principal aim of DEMETER was to develop the concept of multi-model ensemble prediction by installing a number of state-of-the-art global coupled ocean–atmosphere models on a single supercomputer, and to produce a series of six-month multi-model ensemble hindcasts with common archiving and common diagnostic softwares. More information about the project is available on the ECMWF web site at http://www.ecmwf.int/research/demeter.

The DEMETER system comprises seven global coupled ocean–atmosphere models. The modelling partners are: the European Centre for Research and Advanced Training in Scientific Computation (CERFACS), France; ECMWF, International Organization; Istituto Nazionale de Geofisica e Vulcanologia (INGV), Italy; Laboratoire d'Océanographie Dynamique et de Climatologie (LODYC), France; Centre National de Recherches Météorologiques (CNRM), Météo-France, France; the Meteorological Office, UK (UKMO); Max-Planck-Institut für Meteorologie (MPI), Germany. The characteristics of the different coupled models are described and summarized in Table 1 (Palmer et al., 2004). Uncertainties in the initial conditions are represented through an ensemble of nine different ocean initial conditions (for each model, except that of the MPI). Three different ocean analyses are created. A control ocean analysis is forced with momentum, heat and mass flux data from ERA40, and two perturbed ocean analyses are created by adding daily wind stress perturbations to the ERA40 momentum fluxes. The wind stress perturbations are randomly taken from a set of monthly differences between two quasi-independent analyses. In addition, four sea surface temperature (SST) perturbations are added and subtracted at the start of the hindcasts in order to represent the uncertainty in SSTs. As in the case of the wind perturbations, the SST perturbations are based on differences between two quasi-independent SST analyses. Atmospheric and land surface initial conditions are taken directly from ERA40. A separate ensemble initialization procedure is used for the MPI model. Ocean data assimilation has been used in the Met Office experiment after 1987 only.

The integrations are started four times per year on 1 February, 1 May, 1 August and 1 November. Each model produces a nine-member ensemble hindcast and is integrated for six months. The models cover different periods between 1958–2001 and 1980–2001. The periods considered in the present study are 1958–2001 for ECMWF and CNRM, 1959–2001 for UKMO, 1969–2001 for MPI, 1974–2001 for LODYC and 1987–2001 for CERFACS and INGV (CERFACS and INGV simulations were extended to 1980–2001 and 1973–2001 after the present study was made).

The analysis is performed for each of the seven models separately and a multi-model ensemble based on three models (ECMWF, UKMO, CNRM) which all covered the 1959–2001 period, a long period and comparable to the ERA40 period. The resolution used for the model data is 2.5°, which corresponds to the best resolution (without interpolation) common to every model. The analysis of the winter atmospheric variability simulated by the seasonal forecasting models is investigated using December, January and February monthly means from simulations initialized in November. The anomalies are based on individual models climatologies. ERA40 and DEMETER data come from the ECMWF Meteorological Archival and Retrieval System (MARS). They are also available on the ECMWF data web site (http://www.ecmwf.int/research/demeter/data).

Monthly winter pressure fields are considered to analyse the low-frequency climate variability over the NAE region. The following method is used for both ERA40 and the models from DEMETER in order to allow a comparison. A preliminary step consists of an EOF analysis to characterize the variability with a linear method. Then, a non-linear approach is adopted: climate regimes are determined using cluster analysis. A large number of clustering algorithms have been used in many meteorological applications. All these methods depend on the particular type of investigation that is carried out. Cluster analysis is a way to create groups of objects, or clusters, in such a way that the profiles of objects in the same cluster are very similar and the profiles of objects in different clusters are quite distinct. This is based on a similarity criterion inside each group and a dissimilarity criterion between two distinct groups. There are two types of schemes, namely hierarchical and partitional methods. Hierarchical methods are often ascending and form little groups in which inter-distance is as small as possible; they then gather these little groups forming a growing aggregation tree. Partitional methods perform iteratively the classification from randomly predefined initial elements according to a given number k of clusters. In all classifications, each cluster is defined by its centroid, which is the average value of the cluster's elements. Here, the average value is a temporal mean. Before performing cluster analysis, EOF filtering is performed on data to eliminate data noise and to keep climatic variance only. The filtering level is 95%, which corresponds in most cases to about 10 EOFs.

Table 1. Combinations of atmosphere and ocean models used by the seven partners contributing with coupled models to DEMETER (Palmer et al. 2004). The resolution of the models and the initialization strategy is also outlined. The modelling partners are CERFACS, ECMWF, INGV, LODYC, Météo-France, UKMO and MPI

	CERFACS	ECMWF	INGV	LODYC	Météo-France	UKMO	MPI
Atmosphere component	ARPEGE	IFS	ECHAM-4	IFS	ARPEGE	HadAM3	ECHAM-5
Resolution	T63 31 levels	T95 40 levels	T42 19 levels	T95 40 levels	T63 31 levels	2.5° × 3.75° 19 levels	T42 19 levels
Atmosphere initial conditions	ERA40	ERA40	Coupled AMIP-type experiment	ERA40	ERA40	ERA40	Coupled run relaxed to observed SSTs
Reference	Déqué (2001)	Gregory et al. (2000)	Roeckner (1996)	Gregory et al. (2000)	Déqué (2001)	Pope et al. (2000)	Roeckner (1996)
Ocean component	OPA 8.2	HOPE-E	OPA 8.1	OPA 8.2	OPA 8.0	GloSea OGCM, based on HadCM3	MPI-OM1
Resolution	2.0° × 2.0° 31 levels	1.4° × 0.3° –1.4° 29 levels	2.0° × 0.5° –1.5° 31 levels	2.0° × 2.0° 31 levels	182 GP × 152 GP 31 levels	1.25° × 0.3° –1.25° 40 levels	2.5° × 0.5° –2.5° 23 levels
Ocean initial conditions	Ocean analyses forced by ERA40	Ocean analyses forced by ERA40	Ocean analyses forced by ERA40	Ocean analyses forced by ERA40	Ocean analyses forced by ERA40	Ocean analyses forced by ERA40	Coupled run relaxed to observed SSTs
Reference	Delecluse and Madec (1999)	Wolff et al. (1997)	Madec et al. 1998	Delecluse and Madec (1999)	Madec et al. (1997)	Gordon et al. (2000)	Marsland et al. (2003)
Ensemble generation	Wind stress and SST perturbations	Wind stress and SST perturbations	Wind stress and SST perturbations	Wind stress and SST perturbations	Wind stress and SST perturbations	Wind stress and SST perturbations	Nine different atmospheric conditions from the coupled initialization run (lagged method)

The results presented here are obtained with a recursive non-hierarchical method, which is known as the dynamic cluster or *k*-means method (Diday and Simon, 1976). Results are also validated by the Ward classification algorithm (Ward, 1963). This hierarchical method gives similar results. The *k*-means method is preferred here because it classifies each element in the cluster whose centroid is the closest to the element (and this property could be used for forecasting purposes) but some elements that are very close can be classified in two different clusters. As this problem concerns only few elements that are close to the limit between two clusters, it implies no significant impact on the results. In both corresponding algorithms, the number of clusters has to be fixed a priori. So the classification is performed for different numbers of clusters, and then some significance tests are performed on each cluster. Student (T) and Fisher (F) tests are performed on cluster's mean and variance respectively at 95% confidence level to yield the regions where one cluster is significantly different from the total sample. The larger the significant zones are, the better the classification is. The other test used to determine the number of clusters is to calculate the correlation coefficient for each couple of centroids. If high, this means that the algorithm makes one cluster to be divided into two. Tests with the classifiability index (Michelangeli et al., 1995) are not performed because the algorithms used always give the same partition for a given number of clusters (the number of replications with different sets of randomly predefined initial elements and, for each replication, the number of iterations till convergence are high enough for such a result). Also important is the choice of the metrics used to calculate the distance between individual members and centroids. Euclidean distance is chosen, which gives coherent results. Finally, the analysis gives a partition of the members in some groups and the number of groups.

The Brier score (Brier, 1950) is used to evaluate the performances of the models to simulate the ERA40 variability. It is essentially the mean square error of the probabilistic forecasts (Wilks, 1995) defined by

$$\mathrm{BS} = \frac{1}{N_{\mathrm{ens}}} \sum_{i=1}^{N_{\mathrm{ens}}} (p_i - v_i)^2, \quad 0 \le p_i \le 1, \quad v_i \in \{0, 1\} \tag{1}$$

where p_i is the forecast probability for a given event E in the ith forecasts and $v_i = 1$ or 0 whether E occurs or not in the ith verification ($i = 1, \ldots, N_{\mathrm{ens}}$). The N_{ens} forecasts correspond to different times and/or grid points. The Brier score is always positive and equal to zero for a perfect forecast. The lower the Brier score, the better the forecast is. The Brier skill score is defined by

$$\mathrm{BSS} = 1 - \mathrm{BS}/\mathrm{BScli}, \tag{2}$$

where BScli is the Brier score of the climatological forecast. Thus, the forecasts bring information compared to climatology if the Brier skill score is positive. The Brier score and its decomposition in terms of reliability, resolution and uncertainty (Murphy, 1973) are usually associated with the reliability diagram (Wilks, 1995) that compares the observed frequency and the forecast probability (of a given event E).

The temperature impacts of climate regimes are described using different methods. The first representation consists of composites. They are based on the partition of the different winter months in the regimes defined by the cluster analysis on pressure data. ERA40 cluster partition is used for ERA40 composites; model cluster partition is used for model composites. The temperature composites of each cluster are defined as the mean temperature field of the representative months of the considered cluster. Only the elements of the cluster that are close enough to the centroid are kept to calculate the composites. This selection removes the members that are close to the limit between two clusters and that are not clearly classified into a specific cluster. Keeping the elements with a correlation to the centroid higher than 50% allows us to obtain a representative sample of the clusters composed of around two-thirds of the members of each cluster. Composites are calculated on a larger region than the cluster analysis itself (90°W–60°E, 15°N–90°N), in order to have a global vision of impacts over Europe. The composites are plotted for temperature anomalies. As the temperature variability is not uniform from region to region (for instance, a 1° temperature anomaly could be more important in regions where temperature is very stable), it is interesting to use some other kind of representation to quantify the temperature impacts of the regimes. One way is to look at the frequency of occurrence of cold or warm events in a particular regime and to compare it to climatology (Plaut and Simonnet, 2001). For this purpose, the local winter monthly mean temperature anomalies are first classified into three terciles that correspond to cold, near-normal and warm events. With this definition, the climatological frequency of occurrence of each of these three events is 33%. Then, the subset of months for which a given regime occurred is selected and the local frequency of each of the previous categories for this subset of months is computed. Most often, this frequency changes and departs from its climatological value of 33%. The plots of frequency occurrence changes are interesting as this change depends on the region considered. Another way of representing this type of phenomenon is to determine for each grid point which regime is favoured in the case of cold or warm events defined by a specific quantile (20% colder or warmer, for instance). These plots are made using at each grid point the subset of months for which temperature is in the specific quantile. In this subset, the number of months in each regime is calculated. For each grid point, the regime that contains the maximum of months and occurs most often is represented, considered as the favoured regime. To quantify by how much these regimes are favoured, we look at the number of each regime occurrences at each grid point and consider that a certain regime is significantly favoured when the percentage of this regime is more than twice the climatological frequency of regime occurrence (given by the partition of the cluster analysis). For these last two composites representations, the quantile limits are arbitrary; different

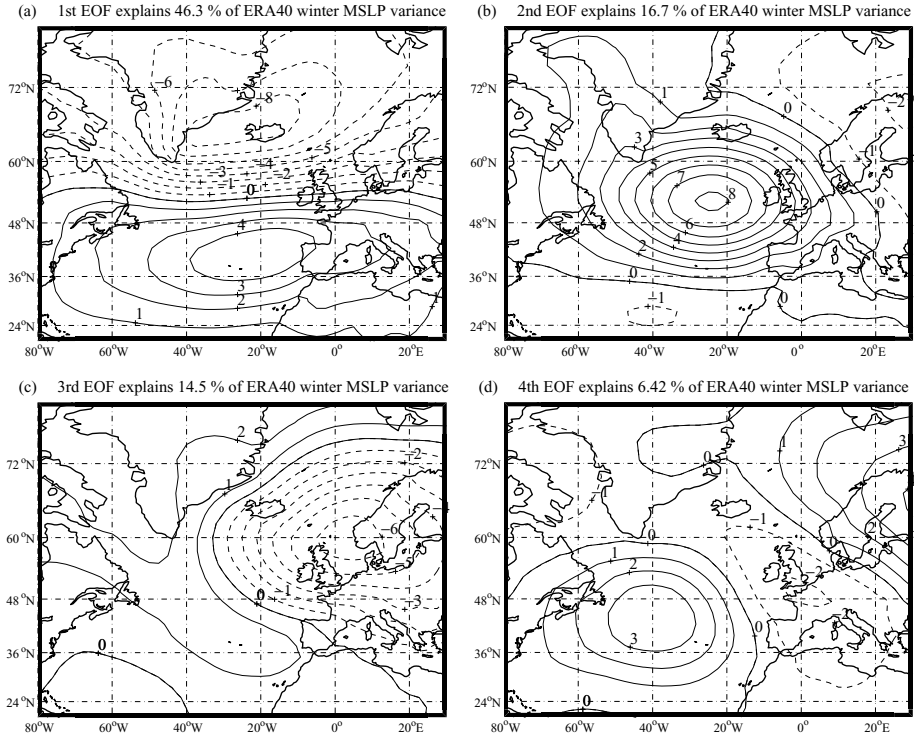

Fig. 1. The four leading EOFs over the NAE region using ERA40 reanalysis monthly mean DJF MSLP data over 1958–2001. Contour interval is 1 hPa.

thresholds are used for comparison and validation of the coherence of results.

3. Climate regimes observed in ERA40 reanalysis

The preliminary step consists of an EOF analysis of monthly mean pressure fields. This first approach aims at characterizing the monthly atmospheric variability, giving some first elements of comparison for Section 4 where the atmospheric variability of the DEMETER models is compared to that of ERA40. As mentioned in many studies on NAE pressure variability (e.g. Hurrell et al., 2003), the leading EOF (Fig. 1a) captures the NAO and explains 46% of the variability. The second EOF (Fig. 1b) corresponds to a pressure anomaly in the North Atlantic basin. The third and fourth EOFs (Figs. 1c and 1d) exhibit extended anomalies from Greenland to the Iberian Peninsula surrounded by opposite sign anomalies over Scandinavia and the Atlantic. The second and third EOFs explain also an important part of winter MSLP variability, 16.7% and 14.5% of the variance, respectively (Figs. 1b and 1c). The fifth and following EOFs (figures not shown) explain less than 5% of variance and 95% of winter MSLP variance is explained by nine EOFs. The analysis of subsamples (parts of the 1958–2001 period) confirms the results with similar EOFs, as does the analysis of NAE regions defined by slightly different latitude and longitude limits.

The cluster analysis of ERA40 data shows that the winter atmospheric variability at the monthly time-scale is multimodal (as Cassou et al., 2004a showed for NCEP reanalysis data). There are four climate regimes defined by their pressure anomalies

Table 2. Correlation coefficients (in %) between the DEMETER model pressure EOFs and the corresponding ERA40 EOFs. The three-model simulation is based on UKMO, ECMWF and CNRM simulations over the 1959–2001 period

	ECMWF	UKMO	CNRM	SMPI	LODYC	INGV	CERFACS	Three-model
First EOF	99	99	93	98	99	99	93	98
Second EOF	36	97	36	72	64	71	46	64
Third EOF	55	97	53	79	73	77	65	74
Fourth EOF	95	95	84	92	97	87	83	95

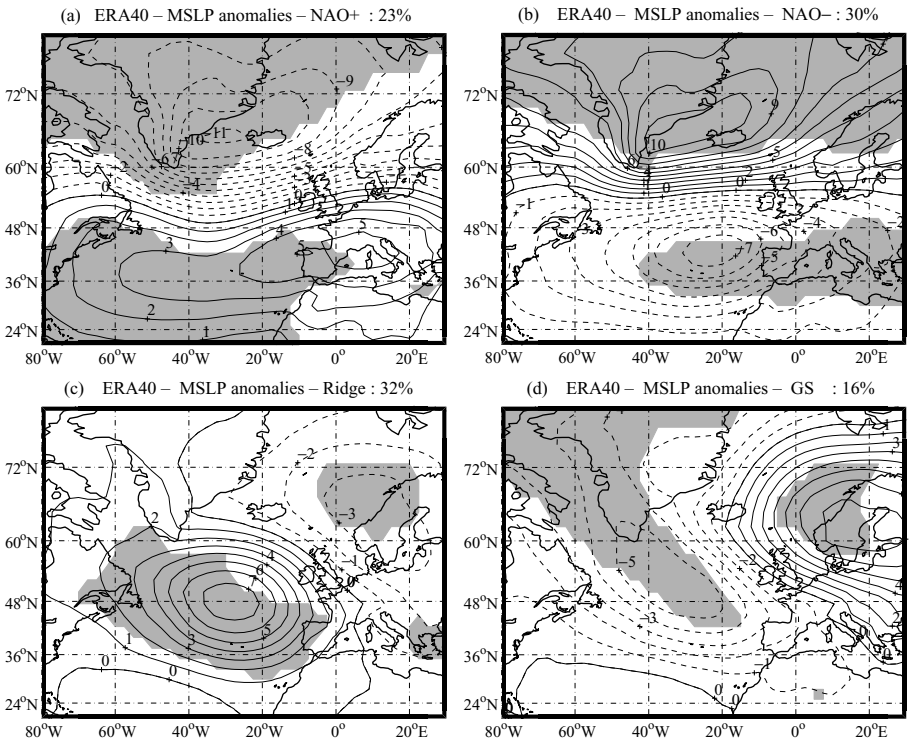

Fig. 2. The four climate regimes obtained with *k*-means cluster analysis on 1958–2001 monthly mean DJF MSLP fields over the NAE region from ERA40 reanalysis. Pressure anomaly centroids are given for NAO+ (a), NAO− (b), Ridge (c) and GS (d) regimes. Shaded areas exceed the 95% confidence level using *T* and F statistics. The global population of a given cluster over the whole period is given by the percentage at the top right of each corresponding figure. Contour interval is 1 hPa.

centroids (Fig. 2); significant areas are shaded and correspond to high-intensity anomalies. The first two clusters (Figs. 2a and 2b) capture the positive and negative NAO phases, respectively, and are called NAO+ and NAO−. NAO+ is characterized by the zonal reinforcement of the Icelandic low and Azores high, and consequently a reinforcement of westerlies. The third cluster (Fig. 2c) is called Ridge, as it displays a strong anticyclonic ridge over the North Atlantic basin with a small negative anomaly over Scandinavia. The fourth cluster (Fig. 2d) exhibits a zonal pressure dipole between Greenland and Scandinavia (GS); the negative pressure anomaly extends towards the Iberian Peninsula, and this GS mode corresponds to anticyclonic blocking.

The partition of the winter months into the four regimes is given by the time history of the occurrence of the regimes (Fig. 3). This figure gives for each winter the number of months in each regime (as in Cassou et al., 2004a) and compares the NAO regimes occurrence to the winter mean NAO index (data from the Climate Research Unit, University of East Anglia) and the projection coefficient of each winter pressure anomaly field on the leading DJF MSLP anomaly EOF (Fig. 1a). The regime partition is very coherent with these two indices.

In order to optimize the number of clusters, the analysis is repeated with two to six clusters (figures not shown). The two-cluster partition yields the two NAO phases. The third mode that appears in a three-cluster partition is defined by a positive pressure anomaly in the North Atlantic, centred west of Great Britain. In both these partitions, several elements are negatively correlated to the centroid of their cluster and the significant areas of the centroids are smaller than those of the four regimes defined above. The five-cluster solution adds another pattern of NAO−, and both NAO− clusters are correlated at 80%. With a six-cluster partition, the same problem appears for NAO+. Finally, the four-cluster analysis brings to light new modes (compared to the two-cluster and three-cluster partitions) that are under 30% correlated. The five-cluster and six-cluster analyses only split the NAO regimes. So the classification of atmospheric pressure states is best represented by four regimes. This study may imply that the NAO− intravariability is relatively high. However, further work shows that this variability is similar or higher in other modes (as shown by the composites building in Section 5). Cluster analysis aims to split elements that are not similar but also gathers elements that are very similar. So, the NAO− splitting rather comes from many NAO− elements that appear to be very similar to one of two NAO− patterns (which are even relatively close and differ slightly by the position of the centres of actions).

The four variability modes are linked with the leading EOFs provided by the EOF analysis presented at the beginning of this section. As the signs of the EOFs are arbitrary, the two NAO modes are both represented by the first EOF. The Ridge mode

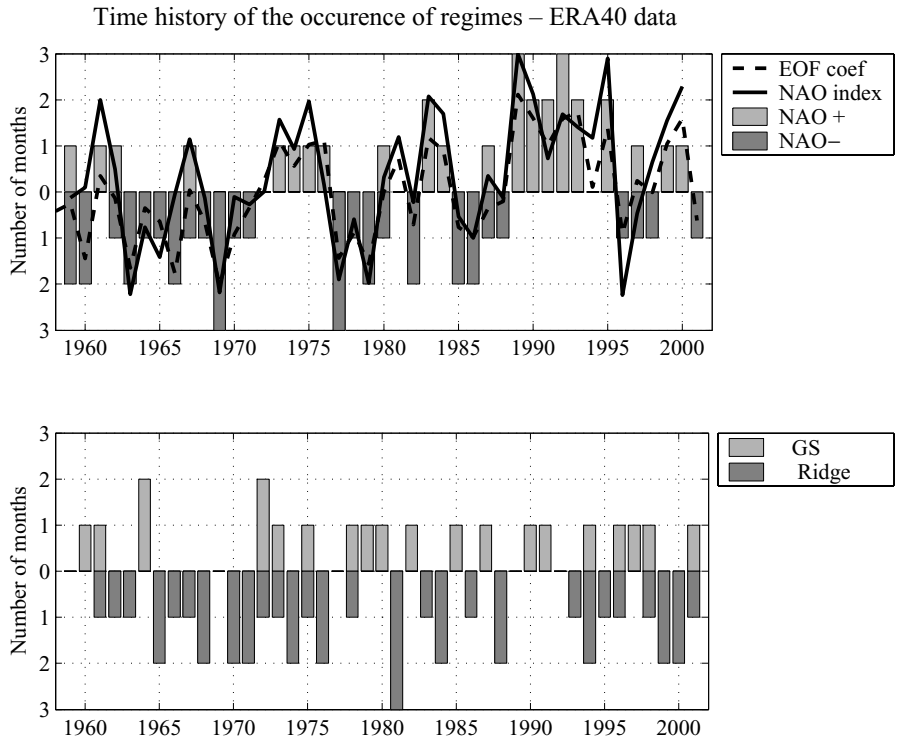

Fig. 3. Time history of the occurrence for the NAO and the Ridge/GS regime. The vertical bars give the number of months relative to each winter in each regime. The solid line denotes the winter mean NAO index (data from Climate Research Unit, University of East Anglia) and the dashed line denotes the projection coefficient of each winter on the leading DJF MSLP EOF.

can be recognized in the second EOF; the pressure anomaly patterns in the North Atlantic basin are very close. At last, the anomaly extension from Greenland to the Iberian Peninsula of the GS mode is linked with the third and fourth EOFs. Thus, the cluster analysis exhibits NAO phases that are not exactly symmetrical, which was not thrown into relief by EOF analysis. NAO+ and NAO− centroids are slightly different in terms of pattern and intensity. Thus, in the case of NAO+, the westerlies anomaly is curved and directed north-eastward over Europe, while it is more zonal in case of NAO−. This is due to the extension of the southern centre from the Azores towards the east. This extension may be linked with anthropogenic forcing (Ulbrich and Christoph, 1999) and this hypothesis is coherent with the increasing frequency of occurrence of NAO+ regimes in the 1980s and 1990s (Fig. 3), which is connected with the observed upward NAO index trend (Hurrell, 1995). There are more details on these points in Cassou et al. (2004a).

The classification of atmospheric variability in four regimes is robust because validated by different complementary calculations. The cluster analysis performed on the NCEP reanalysis (as in Cassou et al., 2004a) yields the same four regimes defined by four centroids that are very close to those of ERA40 data (correlations between each pair of modes are up to 97%). The small differences come from the data periods that are slightly different and from the small distance between the two data sets on the common period. Moreover, for the common period, the partition of months in the different regimes is very similar: only three months over 132 are affected in different regimes and these months are in fact close to the limit between the two regimes. This result is also a statistical validation, as a robust classification should give the same results for slightly perturbed data. The classification of ERA40 data from parts of the 1958–2001 period also exhibits the same four regimes with once again only slight differences between centroids and concerning the partition. Another confirmation comes from the Ward method, which gives similar results for both NCEP and ERA40 data sets. The cluster analysis is also performed on Z500 monthly anomalies (figures not shown), giving again a very similar four-cluster partition, for both ERA40 and NCEP data. The four centroid patterns can be easily associated with those of the MSLP, which means that the atmospheric large-scale pressure states are well described by four regimes. In fact, in all these validations, four regimes appear and most of the differences come from the few months that are not clearly in one regime and whose regime depends on the parameters voluntarily changed. These different partitions impact directly the centroid patterns. At last, the cluster analysis performed on extended winter (from November to March) gives the same four regimes. As the November and March pressure anomalies are weaker compared to the winter months, the study is carried out on winter (DJF) only. All these validations largely confirm the clustering partition of winter monthly atmospheric variability into four regimes.

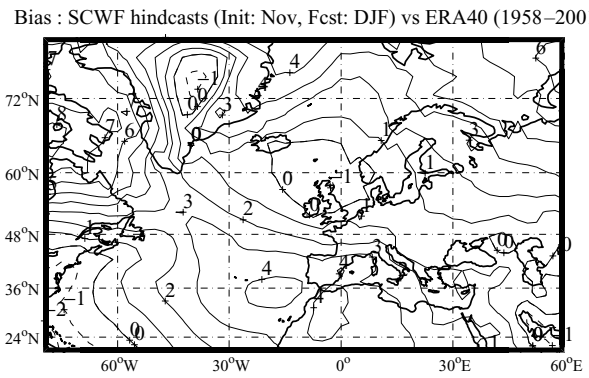

Fig. 4. Mean bias over DJF months between 1958–2001 ECMWF nine-member simulations started on 1 November and the corresponding ERA40 data. Contour interval is 1 hPa.

4. Climate regimes simulated by the DEMETER models

The winter atmospheric variability of DEMETER seasonal hindcasts is studied using the monthly pressure anomalies calculated with respect to the monthly climatologies of each individual model, in order to remove the model biases with respect to ERA40. Biases depend on models, regions, seasons and forecast periods. For instance, the mean bias over DJF months between 1958–2001 ECMWF simulations started in November and the corresponding ERA40 data (Fig. 4) is positive around the Azores where it reaches 4 hPa, slightly negative over Greenland and near zero between Iceland and Great Britain. On the other hand, the bias between CNRM simulations and ERA40 (figure not shown) is negative over Great Britain, positive over the Mediterranean Sea and reaches 6 hPa.

To take into account the whole variability of the model simulations, the analysis is applied to the winter months from the nine-member ensemble simulations initiated in November. For the ECMWF simulations, which cover the 1958–2001 period, there are 1188 members to classify (three months per winter, 44 winters and nine simulations for each start date).

In this section, we present results of the EOF and cluster analysis applied on DEMETER simulations, with the objective of determining if winter climate variability is correctly simulated by the different models of the DEMETER seasonal forecasting system. To that purpose, results are compared to those obtained in Section 3 with ERA40 data; the methods and criteria used are those introduced in Sections 2 and 3.

As for ERA40, winter atmospheric variability simulated by the models is first studied by an EOF analysis. Tables 2 and 3 quantify the differences between the four leading EOFs of the models (Fig. 5 for ECMWF) and the four corresponding EOFs obtained with ERA40 data (Fig. 1). Table 2 compares EOF patterns and structures by giving the correlation coefficient between models and ERA40 EOFs. For every single model and for the three-model ensemble (simulations from CNRM, UKMO and ECMWF), the leading EOF is highly correlated with ERA40 first EOF. The models are able to capture the NAO variability as the leading EOF is always characterized by anomalies over Iceland or Greenland and anomalies of opposite sign over the Azores. The small differences come from the positions of the centres of action, the pattern of the anomalies and the percentage of explained variance. Thus, the west flux anomaly associated with the NAO EOF is directed more northward in ECMWF simulations than in ERA40. The second EOF is not as well simulated especially by ECMWF (Fig. 5b) and CNRM, which displace the anomaly over the North Atlantic towards Great Britain. Another interesting point is the high scores of the UKMO model whose four EOFs appear to be highly correlated (up to 95%) with ERA40 EOFs. Table 3 shows that the percentages of variability explained by the EOFs of the models are not uniform but of the order of those of ERA40. Indeed, for every single model and the three-model ensemble, the leading EOF explains 40–50% of winter MSLP variance (46% for ERA40), the second and third EOFs explain 10–20% (16% and 15% for ERA40), and the following less than 8% (less than 7% for ERA40). Finally, the main observed patterns of pressure variability are found in the different models of the DEMETER system. However, the biases between models and ERA40 variability are not totally thrown into relief by this study, as they are contained partly by each EOF and each corresponding percentage of explained variance. Thus, they will be commented on in the following from the point of view of climate regimes.

The winter atmospheric variability simulated by the models is then studied using cluster analysis. As for ERA40, the analysis

Table 3. MSLP winter variance (in %) explained by the four leading EOFs in the ERA40 reanalysis and in DEMETER simulations. The three-model simulation is based on UKMO, ECMWF and CNRM simulations over the 1959–2001 period

	ERA40	ECMWF	UKMO	CNRM	SMPI	LODYC	INGV	CERFACS	Three-model
First EOF	46.3	39.8	43.2	49.0	44.8	43.3	46.5	46.6	42.8
Second EOF	16.7	17.4	15.7	17.4	21.0	16.3	17.3	18.4	16.4
Third EOF	14.5	16	11.0	10.1	11.7	14.3	12.0	10.3	13.0
Fourth EOF	6.4	7.5	7.9	5.9	4.9	7.4	6.5	6.9	7.1

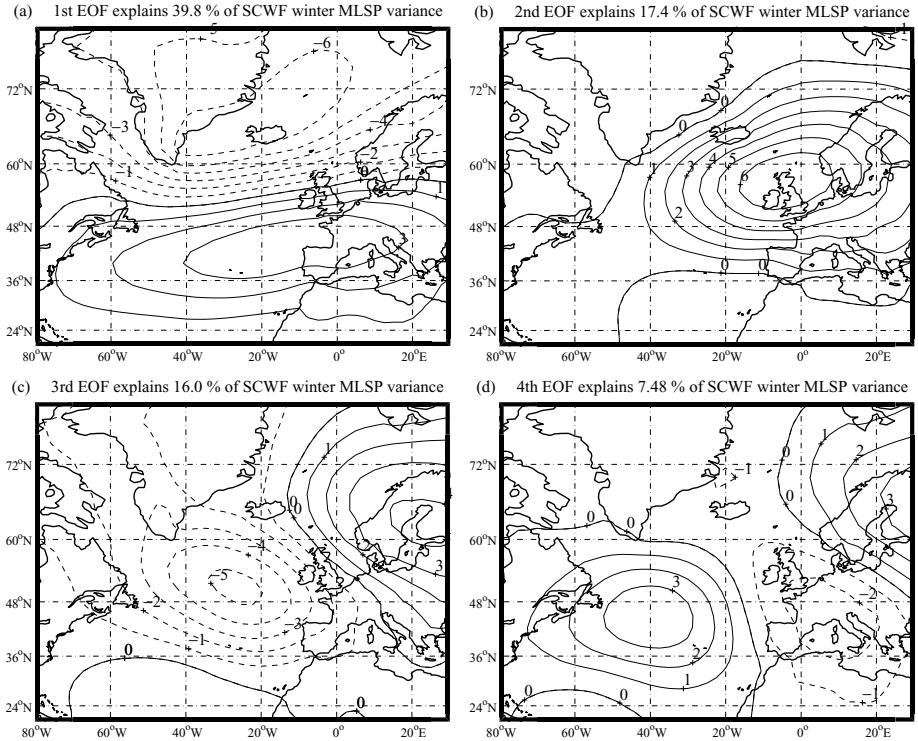

Fig. 5. Same as Fig. 1 but for 1958–2001 ECMWF nine-member simulations started on 1 November.

performed on ECMWF simulations yields four regimes defined by four distinct centroids (Fig. 6). The number of clusters is determined by the same process used for ERA40 and the same arguments are used to determine the number of regimes. For instance, the five-cluster partition exhibits two NAO− modes whose centroids are highly correlated. Interestingly, the supplementary regime is the same as for ERA40. The ECMWF regime centroids (Fig. 6) are highly correlated to the four ERA40 centroids (Fig. 2), as shown by the correlation coefficients given in Table 4. The correlation is 95% for the NAO+ regime, 98% for NAO− and 85% for the Ridge and GS regimes. There are only small differences in patterns and intensities, and the areas of high variability are slightly displaced. Concerning GS (Fig. 6d), the extension of the low pressure towards the south-east is less pronounced than for ERA40, which reduces the northern flux anomaly intensity going round Western Europe. NAO regimes (Figs. 6a and b) are not symmetric. So the extension of the southern centre from the Azores towards the east is well simulated even if the displacement is smaller than in ERA40. The NAO+ region of weak anomalies located between the pressure anomalies is zonal, which means that the western flux anomaly is zonal instead of north-eastward in ERA40 case. At last, the Ridge low pressure over Scandinavia is displaced slightly eastward (Fig. 6d). For the four centroids, significant areas are quite large compared to those of ERA40. This is due to the ensemble size, which is nine times larger, and gives a more important statistical significance to the results.

The cluster analysis performed on the six other DEMETER models also exhibits four regimes. The two NAO phases are well simulated. The position and the intensity of the characteristic centres (where anomalies are high) of the centroids (figures not shown) vary from model to model, but the NAO regimes simulated by the models are all well correlated with ERA40 NAO regimes (Table 4). The correlation between the NAO+ centroid of each model and ERA40 is higher than 92% and higher than 97% for NAO−. For the CNRM model, the southern centres of action of NAO regimes are both displaced northward compared to ERA40, which leads to a northward displacement of the western flux anomalies. For the other models, the differences also lead to slight changes of direction and intensity of the western flux anomalies. Concerning the two other modes, they are a little more different compared to the Ridge and GS regimes obtained with the ERA40 cluster analysis. We called these two modes HP–GB and BP–GB because they are characterized respectively by high and low pressures over Great Britain (or slightly westward, depending on the model considered) and they are nearly symmetric. Figure 7 presents the HP–GB (Fig. 7a) and BP–GB (Fig. 7b) centroids obtained for the UKMO model. These two modes can be compared to Ridge and GS as Ridge presents a high pressure and GS a low pressure in the Atlantic. However, the differences between ERA40 clusters and these new modes are not negligible in particular for GS and BP–GB. The BP–GB negative pressure anomaly is circular in the case of BP–GB instead of a south-eastward

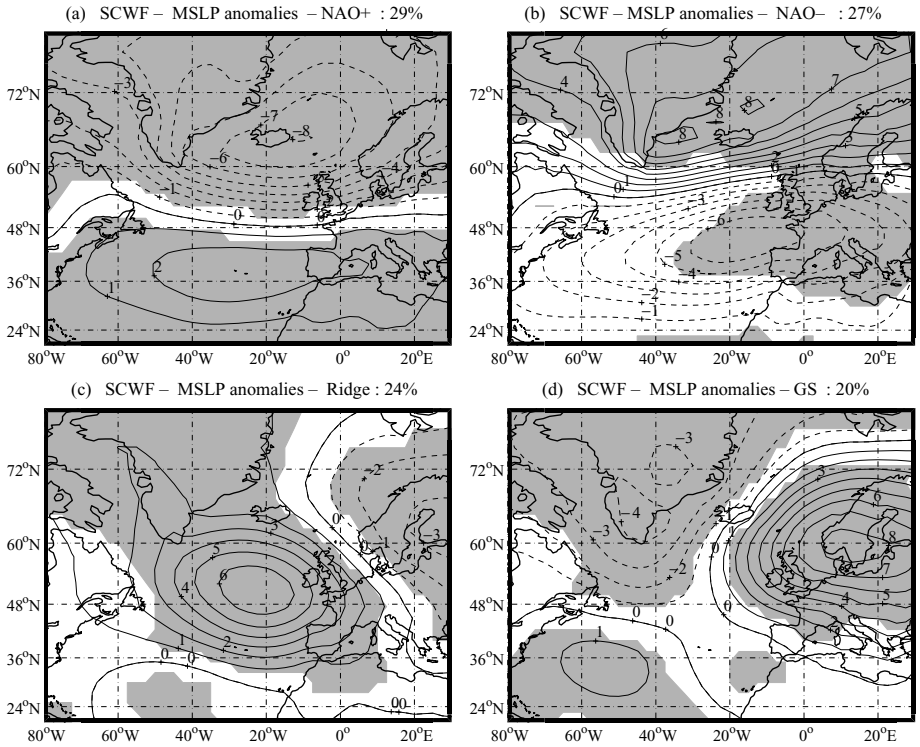

Fig. 6. Same as Fig. 2 but for 1958–2001 ECMWF nine-member simulations started on 1 November.

Table 4. Correlations (in %) between the DEMETER model pressure centroids and the corresponding ERA40 centroids. The HP–GB and BP–GB modes of DEMETER models (except ECMWF) are compared to Ridge and GS, respectively. The three-model centroids are based on analysis of UKMO, ECMWF and CNRM simulations over the 1959–2001 period

	ECMWF	UKMO	CNRM	LODYC	SMPI	INGV	CERFACS	Three-model
NAO+	95	99	92	96	95	95	94	98
NAO−	98	99	97	99	99	99	98	99
Ridge	85	64	0	21	22	17	26	18
GS	85	37	−31	19	5	−6	−5	−24

extension coming from Greenland, so that pressure anomalies over Greenland are quite reduced. These pattern differences induce changes of directions of airmass fluxes, which are more circular, the position of the round circulation varying from model to model depending on the position of the low-pressure anomaly. The correlation between HP–GB and Ridge varies from model to model from 0% to 60% and the correlation between BP–GB and GS varies from −30% to 30% (Table 4). These results are coherent with the results of the weather regimes simulated by the ARPEGE model (Terray and Cassou, 2002; Cassou et al., 2004a). Atmospheric general circulation models (AGCMs) are able to capture the leading NAO+ and NAO− weather regimes, while the third and fourth regimes are more symmetrical with strong circulation over the North Sea. Similar results are obtained here for the climate regimes simulated by the seasonal forecasting coupled models of the DEMETER system. This concerns all models (especially Météo-France and CERFACS, which used the ARPEGE model for the atmosphere component) except ECMWF whose clusters 3 and 4 are very close to ERA40 clusters, whereas they are rather different for the six other models. In both ECMWF and LODYC simulations, the Integrated Forecast System (IFS) model is used for the atmospheric component; however, LODYC does not simulate correctly the four regimes. It shows that the oceanic component and other model characteristics have high impacts on simulations results. The stochastic physics scheme is an originality of ECMWF model, which might explain the fact that ECMWF simulates correctly the four regimes. However, further analysis should be carried out

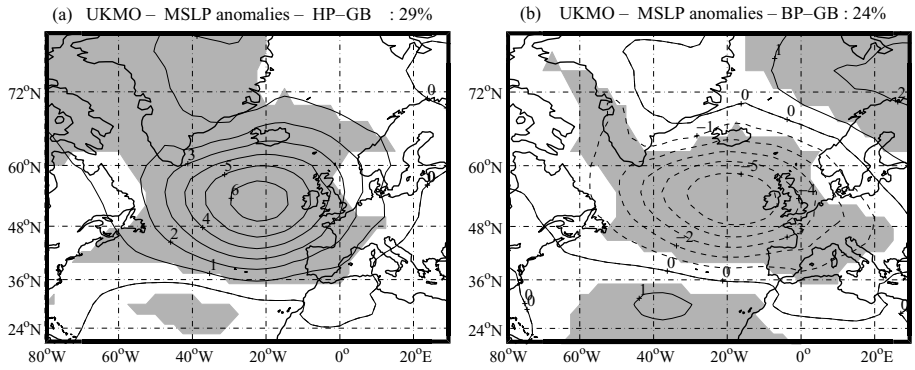

Fig. 7. Same as Fig. 2 but for 1959–2001 UKMO nine-member simulations started on 1 November. Two of the four regimes are displayed: HP–GB (a) and BP–GB (b). NAO regimes are not shown.

to try explaining clearly these discrepancies. It is interesting to mention that although the four leading EOFs simulated by the UKMO model are very close to ERA40, ECMWF regimes are closer to ERA40 than those of UKMO. Indeed, the structures of the four leading EOFs do not represent the whole variability. The following EOFs, (even if they capture less than 5% of MSLP variability) and the percentages of variance explained by each EOF (Table 2) are also important. The distance between UKMO regimes and ERA40 regimes comes, at least in part, from these differences.

To estimate the multi-model potential, the cluster analysis is also performed on the simulations from ECMWF, CNRM and UKMO (as a whole) over the 1959–2001 period as these three models covered this period, which is comparable to the ERA40 period. The analysis logically yields four regimes: the two NAO phases, HP–GB and BP–GB, which are slightly different from the centroids of each model. The results reflect the three single-model analyses. HP–GB and BP–GB appear rather than GS and Ridge, because they are simulated by both CNRM and UKMO.

For all these experiments, the results are, as for ERA40, confirmed by both clustering methods (Ward and *k*-means) performed on both MSLP and Z500, and on subsamples of members. These different tests confirm the same number of clusters and partition.

Concerning the partition of the elements (DJF months) in the four regimes, the percentages of members in a given cluster vary from model to model and differ from ERA40 too. For ERA40, ECMWF and UKMO, these percentages are mentioned in the top right of the climate regime figures (Figs. 2, 6 and 7). Hence, the dominant regime is not always the same. Even for every single model and the three-model ensemble, the partition is always quite balanced as each of the four regimes contains between 16% and 35% of the total number of elements. However, it is difficult to compare each model with ERA40, as the covered periods are sometimes quite different.

As DEMETER models simulate quite well the atmospheric variability over the NAE region, it is interesting to determine if model simulations allow us to forecast the type of regime for a given date. The cluster analysis of model simulations presented above gives the partition of the DJF months in the four regimes. Then for each forecast DJF month, it is possible to compare the regimes given by the simulations with the regime that really occurred, which is defined by the ERA40 cluster analysis partition represented by the regime chronology (Fig. 3). For this purpose, HP–GB and BP–GB regimes (forecast by DEMETER models except ECMWF) are assumed to correspond to Ridge and GS regimes, respectively. The Brier score is first calculated for the forecasts of each of the four regimes without model calibration for every single model and the December 1958 three-model ensemble. This means, for instance, that the December 1958 nine-member ECMWF simulation from November 1958 partitioned in three regimes (one member in GS, three in NAO− and five in Ridge) by the cluster analysis performed on ECMWF simulations gives the regime forecast probabilities of 1/9 for GS, 3/9 for NAO− and 5/9 for Ridge. These probabilities are then compared to the climatological probabilities of the ERA40 cluster analysis (23% for NAO+, 30% for NAO−, 16% for GS and 32% for Ridge) using the Brier skill score. For the individual dynamical models and the three-model ensemble, the Brier skill scores are slightly negative (around −10% for ECMWF). From this point of view, climatological prediction is more reliable than that of the models. One point may be that the models are not performing enough at the monthly time-scale, as seasonal forecast scores are generally higher for seasonal values. Another point is that the simulated regimes vary from model to model and are more or less correlated with ERA40 regimes, which may not help to forecast the regime that really occurred. For this reason, instead of using the model cluster partition, the model pressure anomalies are projected on the ERA40 regimes centroids to determine the regime forecast by the simulations. However, once again, the Brier skill score is slightly negative. In fact, in all the evaluation methods of the forecast scores described above, the distance or correlation between the members and the centroid of the regime in which they are affected varies and this is not taken into account. Indeed, for instance, for the December 1958 nine-member ECMWF simulation from November 1958,

the three members classified in the NAO− regime are close to the ECMWF NAO− centroid (correlation between 76% and 80%), the member classified in GS is 71% correlated to the GS centroid, and the five members classified in Ridge are differently correlated to that of the Ridge (0%, 5%, 9%, 32% and 72%). To some extent, the NAO− is forecast with a probability larger than 3/9. Moreover, the same problem appears for the ERA40 regimes; when the NAO− regime occurs, it is more or less far from the centroid. To overcome this, some different weightings were considered, but the tests did not manage to throw into relief some positive skill. To summarize, these different experiments show that some scores are negative but the evaluation of the skill of the forecasts regimes is quite complex.

The skill evaluation of the forecast regimes and the analysis of the ensemble simulation partition of the different models in the four regimes also show that members for a given forecast date are always distributed in three or four regimes, which means that the spread of the ensemble is quite large. Indeed, the MSLP anomalies of the nine members are generally structurally quite distinct and the mean standard deviation of the nine members of ECMWF simulations over the NAE region and the 1958–2001 period is 4 hPa. The partition of the model simulations in different regimes reveals that small perturbations in the initial state have important impacts on the simulations as different regimes can be reached. Hence, simulations for a given forecast date are forced by different ocean states (defined by the perturbed initial states) that evolve differently. The climate regimes can be excited by some (previous or simultaneous) SST anomalies in the Tropical and North Atlantic (Cassou et al., 2004a; Cassou et al., 2004b). This explains, at least in part, that different regimes are forecast by the ensemble simulations.

Finally, winter atmospheric variability is globally well captured by DEMETER models with the same number of modes. The ECMWF regimes are very similar to those of ERA40. The other model regimes well represent the two NAO phases, the two other modes being substantially different. No clear explanation of the different results obtained for the ECMWF model with respect to the six others could be found. The fact that ECMWF simulates correctly the four regimes might be due to the stochastic physics scheme, which is an originality of the ECMWF model, but some extra analyses should be made to confirm this assumption. The skill of forecasting which regime will occur seems to be very weak, and further investigation is needed to characterize it more precisely.

5. Temperature impacts of the winter regimes

In this section, we examine the links between the pressure regimes described in Sections 3 and 4 and the associated temperature anomalies. The objective is to determine if the climate regimes correspond to characteristic patterns of temperature. This is the idea of classified and classifying variables (Martineu, 1997; Martineu et al., 1999). If the cluster analysis obtained from MSLP data is robust, it should correspond to distinct and well-separated patterns (composites) of other variables, and cluster analysis performed on other variables should lead to similar partitions.

For this purpose, the temperature impacts of the regimes are investigated using ERA40 data and DEMETER models simulations to describe the observed and simulated impacts. The fields considered are monthly winter anomalies of 850 hPa and 2-m temperature. Globally, the results are very similar for both fields and only the results for T850 are presented here, as they show the large-scale features only.

Temperature composites of the four ERA40 regimes are displayed in Fig. 8. The number X of members that are taken into account to calculate the composite (members whose correlation with centroid is higher than 50%) is compared to the total number Y of elements in the cluster. This X/Y ratio is mentioned in the top right of the plots. The NAO composites (Figs. 8a and b) show that NAO members are highly correlated to their centroids as all the members are considered to calculate the composites. They illustrate the impacts of the NAO described in Hurrell et al. (2003), giving the NAO specific temperature anomalies. The NAO+ regime is characterized by the reinforcement of the Icelandic low and the Azores high, which reinforces the storm track and westerlies that bring warm (and wet) air in northern Europe, as illustrated by the NAO+ T850 composite (Fig. 8a). On the other hand, the NAO− regime is characterized by negative anomalies in southern Europe and negative anomalies over the north-eastern Atlantic (Fig. 8b). The NAO− T850 composite is nearly symmetrical to that of NAO+. In Europe, the limit between positive and negative anomalies is located to the south of France for NAO+, and over France for NAO−. The Ridge regime is characterized by a strong anticyclonic anomaly over the North Atlantic (Fig. 2c), which brings cold air from Greenland to Europe, so that the corresponding composite (Fig. 8c) displays a positive anomaly over central North Atlantic, and negative anomalies around this positive centre (over Greenland, western Europe and the southern North Atlantic). Finally, the anticylconic anomaly over Scandinavia of the GS regime prevents westerlies from reaching Europe and makes them deviate northwestward, giving a GS composite (Fig. 8d) relatively opposed to that of the Ridge, with positive anomalies from Greenland to Scandinavia and over southern North Atlantic, and negative anomalies over the central North Atlantic and eastern Europe. Thus, the four composites are well distinct, which reinforces the validation of the classification of winter atmospheric variability in four regimes. Moreover, the classification is confirmed by the cluster analysis performed on T850 fields, which leads to four centroids very close to the composites described above and a partition similar to that obtained with MSLP.

The plots of the change of frequency occurrence also confirm the tendencies given by the composites. Only one figure (Fig. 9) is given for illustration. In the case of the Ridge regime, the occurrence frequency of lower tercile events departs from its

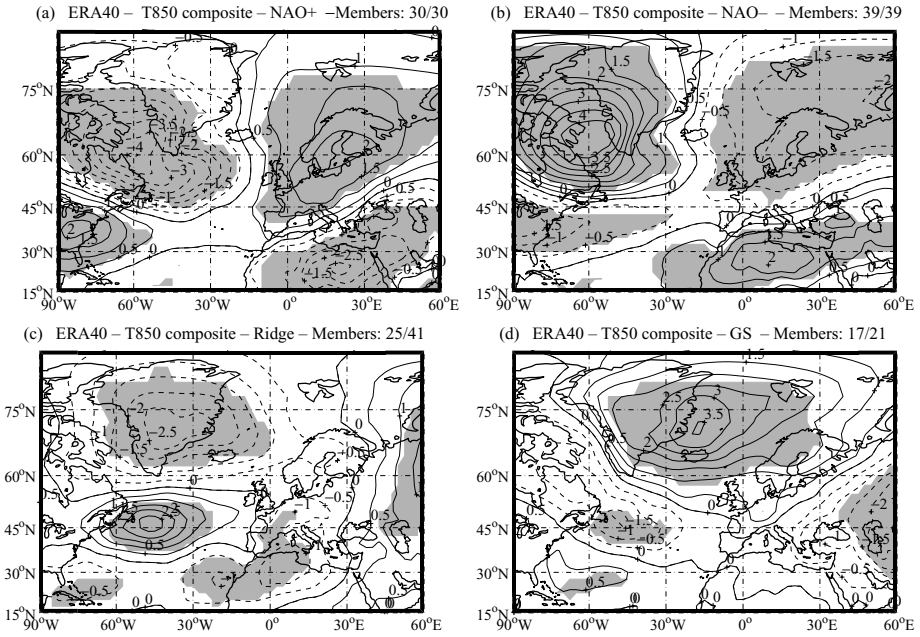

Fig. 8. The four 850-hPa temperature composites that correspond to the four climate regimes provided by *k*-means cluster analysis on 1958–2001 winter pressure over the NAE region from ERA40 reanalysis. NAO+ (a), NAO− (b), Ridge (c) and GS (d) composites are composed by averaging the *X* of *Y* members (winter months) of each cluster that are correlated to their centroids up to 50%; this *X*/*Y* ratio is given at the top right of each corresponding figure. Shaded areas exceed the 95% confidence level using T statistics. Contour interval is 0.5°C.

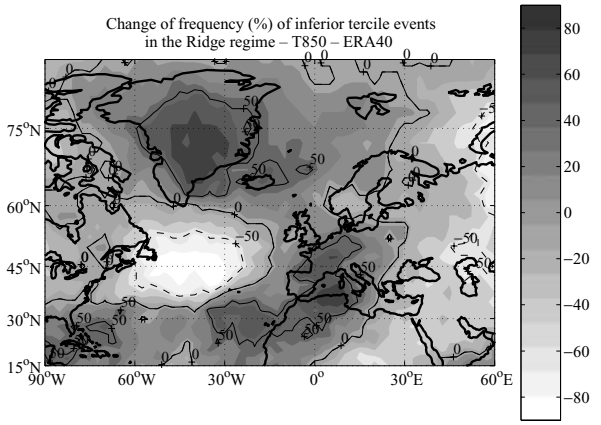

Fig. 9. Change of the frequency occurrence of the T850 lower tercile events in the Ridge regime compared to the climatological frequency (33%). Data used are ERA40 reanalysis.

climatological value of 33% and this change is not uniform in the NAE region (Fig. 9). The frequency is higher than climatology over western Europe and Greenland (change around +50%) and lower than climatology in the Atlantic (change around −80%). In the case of the NAO+ regime, the change of frequency occurrence of cold events (lower tercile) is around −100% over Europe (figure not shown). It is interesting to mention that this change of frequency occurrence is quite uniform over northern Europe while the composite anomalies are not. These plots take into account the local variability. They also throw into relief that the change of frequency of normal events (central tercile) is quite small (under 30% in Europe) for the four regimes, which means that normal events occur with similar probabilities in the four regimes.

Figure 10 shows the favoured regimes in each grid point in the case of cold (Fig. 10a) and warm events (Fig. 10b), defined by the 20% extreme anomalies. The favoured regime is the regime that occurs most often. To quantify by how much these regimes are favoured, the number of occurrences in each regime is calculated for each grid point and is compared to the number of extreme events. A certain regime is significantly favoured when the percentage of this regime is more than twice the climatological frequency occurrence of this regime. The climatological frequency occurrences are given by the partition obtained with the cluster analysis in Section 3: 23% for the NAO+ regime, 30% for NAO−, 31% for Ridge and 16% for GS for ERA40. Significant areas are represented by dotted regions (Figs. 10a and b). For instance, the cold events of northern Europe occur more often during the NAO− regime than in the case of the three other regimes (Fig. 10a), and, as this area is dotted, more than 60% of these cold events correspond to NAO− regimes. Figure 10a also shows that the cold events of south-western Europe occur more often during the Ridge regime, and those of the western Mediterranean during the NAO+ regime. Concerning the warm events, those of northern Europe (France included) occur mainly during the NAO+ regime. The NAO− regime is favoured over North Africa and Mediterranean (Fig. 10b). The

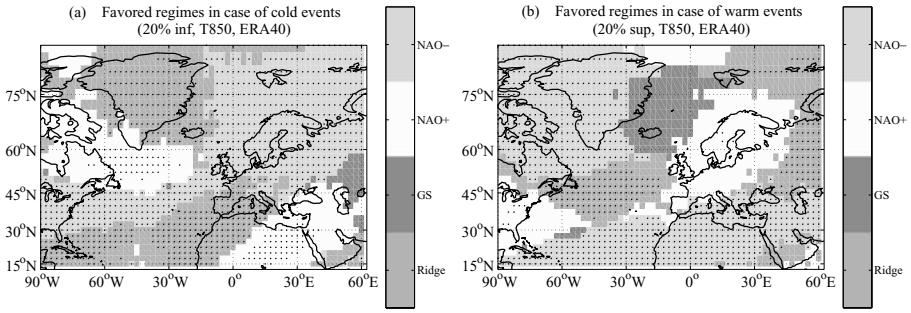

Fig. 10. Favoured regimes in the case of 850-hPa temperature extreme events (ERA40 data). Cold and warm events are defined by the 20% extreme anomalies of winter monthly 850-hPa temperature. At each grid point, specific shading represents the regime that occurred more often than the three others in the case of cold (a) and warm (b) events. Significant areas are dotted.

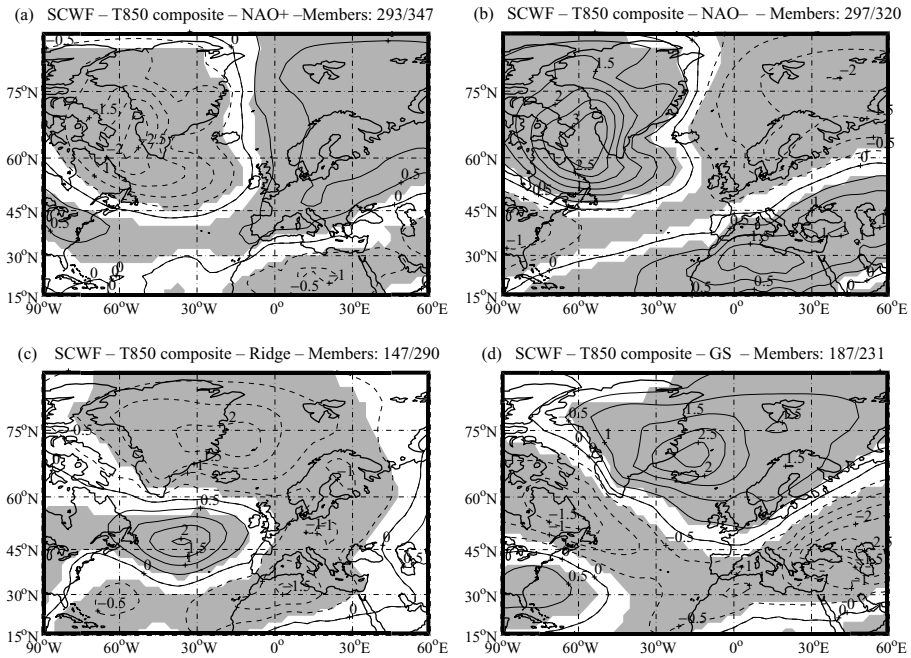

Fig. 11. Same as Fig. 8 but for 1958–2001 ECMWF nine-member simulations started on 1 November.

NAO+ favoured region is less significant, but the percentage of the NAO+ regime is around 55%, which is quite high compared to climatology. Finally, these plots yield clear and distinct regions where one or another regime occurs more often than the others in the case of cold or warm events. As the plots of change of frequency occurrence, they confirm the composites tendencies and give another point of view. In all these calculations, other thresholds (for the definition of cold and warm events quantiles) also give interesting results that yield characteristic regions. They only change the extension of the specific regions. A 5% change in the threshold makes the limits between characteristic zones move from few grid points only, and this change is quasi-null for high-significance zones.

For the ECMWF model, T850 composites (Fig. 11) are very similar to ERA40 composites. Anomalies signs and patterns are well simulated. Only in some regions are the anomaly intensities slightly lower than those of ERA40 composites. This statement concerns more specifically Europe in the NAO+ and GS regimes. This reveals that models slightly underestimate real temperature variability on the monthly time-scale. As for the pressure centroids, areas of significance are larger than for ERA40, which may be due to the ensemble size (nine times bigger for the models than for ERA40). There are some small differences concerning the position of the characteristic anomalies centres, as the southward displacement of the limit between positive and negative anomalies in Europe for the NAO+ composite. The ECMWF favoured regimes of cold and warm events (Fig. 12) are also very close to ERA40 plots (Fig. 10) as they show clear distinct regions where one regime or another is favoured. The main difference concerns the size of the regions where the NAO+ regime is favoured in the case of warm and cold events, which are larger for the ECMWF plots. In fact, these differences come from the frequency occurrence of the NAO+ regime in the ECMWF simulations, which is higher than in ERA40: 29% compared to 23%

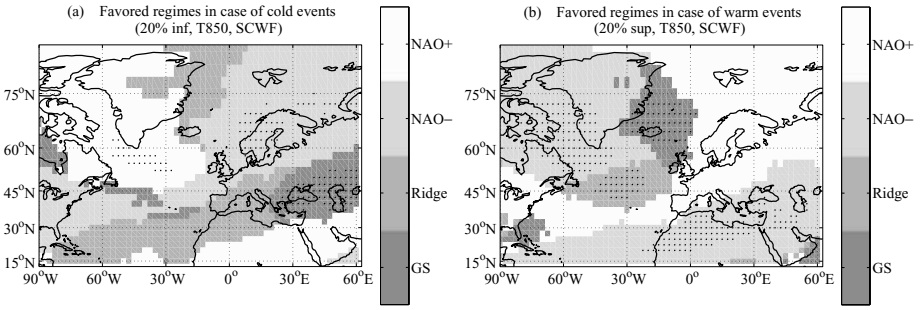

Fig. 12. Same as Fig. 10 but for 1958–2001 ECMWF nine-member simulations started on 1 November.

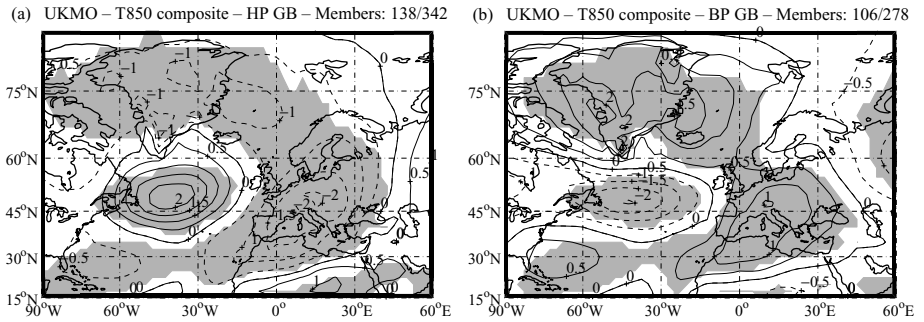

Fig. 13. Same as Fig. 8 but for 1959–2001 UKMO nine-member simulations started on 1 November. Composites are displayed for two of the four regimes: HP–GB (a) and BP–GB (b). NAO composites are not shown.

for ERA40. Significant zones are also less extended than those of ERA40. This suggests that the link between the high-temperature (20% extremes) impacts and the pressure regimes is less clear than in ERA40, although the mean impact (illustrated by the composite results) is clearer. So, in the model simulations, the pressure regimes induce some temperature anomalies but their intensities may be slightly underestimated. These differences may also be due to the different methods used for quantifying the impacts: composites are calculated with members whose correlation to the corresponding centroid is up to 50%, and ERA40 composites take into account more members than ECMWF, for instance. On the other hand, the favoured regime plots include all the members as for ERA40; 20% of the members correspond to (only) 26 members. Thus, the ability to deduce the temperature from the dominant pressure regime is less skilful in the model than in ERA40 but does exist. Indeed, in the case of a warm event, in northern Europe, NAO+ is favoured with a probability of around 50% (which is higher than the climatological probability of 29%). In the case of cold events (Fig. 12a), the favoured areas are not so distinguishable around limits between western Europe regions influenced by Ridge, GS and NAO−. For ECMWF composites, a 5% change in the threshold makes the limits move between characteristic zones from several grid points. Finally, both ECMWF pressure regimes and temperature impacts are close to those of ERA40. The ECMWF model captures the pressure atmospheric variability as well as the link between temperature and pressure fields.

For the six other DEMETER models, the NAO regime composites are very similar to ERA40 and ECMWF (figures not shown). As HP–GB and BP–GB modes are quite different from Ridge and GS, associated composites are also quite different. They globally correspond to those of the Ridge and GS, but they are quite symmetrical, which is consistent with the symmetrical pressure structures of the HP–GB and BP–GB modes (Figs. 7a and b). As for the pressure regimes, differences between GS and BP–GB composites are higher than between Ridge and HP–GB, the circular anticyclonic anomaly of BP–GB inducing some positive anomaly over western Europe. HP–GB and BP–GB composites from the UKMO model are shown as an example (Fig. 13). For these DEMETER models (all but ECMWF), the HP–GB composite (Fig. 13a for UKMO) is characterized by positive anomalies in the North Atlantic, surrounded by negative anomalies over Greenland, western Europe, and subtropical Atlantic and is quite correlated with the Ridge composite. BP–GB (Fig. 13b for UKMO) composites are globally opposed to HP–GB composites but are quite different from GS composites. Thus, the six other DEMETER models are able to simulate some relations between temperature and pressure fields. The simulation of the pressure/temperature link is not as good as for the ECMWF model, but this property results directly from differences between the simulated pressure regimes.

The same analysis is also performed for precipitations (figures not shown). The ERA40 composites display some characteristic anomalies, such as the NAO impacts described by Hurrell et al.

(2003) – some positive anomalies in northern Europe in the case of NAO+ regimes – but the patterns are generally not very clear and the intensity is very small. The point is that precipitation fields are dispersed and the ERA40 data set may not be accurate enough for such an analysis. Concerning models, composites make some characteristic features appear, but they would need to be compared to the composites made with an accurate analysis, such as the GPCP product (Arkin and Xie, 1994) for instance. Moreover, model resolution is too small to correctly represent cloud microphysics and precipitation simulations do not represent local scale variability, so that it is difficult to speculate on the results of these precipitation composites.

6. Summary and perspectives

The monthly atmospheric variability of large-scale pressure fields over the NAE region and the corresponding impacts in temperature are investigated both in the ERA40 reanalysis data set and in the DEMETER seasonal forecasting system.

The observed winter (DJF) atmospheric variability is multimodal. The partition determined by a cluster analysis on sea level pressure anomalies yields four distinct climate regimes. The first two clusters capture the negative and positive phases of the NAO. The third (Ridge) and fourth (GS) clusters display respectively a strong anticyclonic ridge off western Europe and a zonal pressure dipole between Greenland and Scandinavia, with a clear southwestward extension of the low-pressure anomalies towards the Iberian Peninsula. Different tests and calculations show that this partition is very robust. All the regimes are characterized by different and specific patterns of temperature. Indeed, each regime is linked to the change of frequency occurrence of some specific events (20% coldest or warmest events, for example) and this dependency is regional. From another point of view, the impacts of a specific regime in terms of temperature anomalies can be very different from one subregion to another.

The DEMETER seasonal forecasting models are able to reproduce the multimodal variability of the winter atmosphere, with the same number of modes. The four-regime partition is again very robust. For the ECMWF model, the pressure patterns of the regimes and the associated temperature composites are very similar to those obtained with ERA40. For the six other models, the two NAO modes are well reproduced but the two other regimes are more different. No clear reason could be found in this study to explain the differences between ECMWF and the six other models. Further investigation is needed to answer this question. However, the DEMETER system does not allow forecasting the regimes for a given date, and climate regime prediction scores and skill scores are low. Concerning the impacts of regimes on temperature, the DEMETER models are able to reproduce the link between pressure and temperature fields. Temperature impacts in ECMWF hindcasts are closer from ERA40 than in the six other model hindcasts. Lastly, some predictability could arise from reliable seasonal predictions of pressure fields at a monthly time-scale, which should allow us to forecast the type of regime excited and to deduce the corresponding large-scale pattern of temperature anomalies.

The atmospheric variability was also investigated in the other seasons for both ERA40 data and DEMETER hindcasts. NAO-like regimes are found but the multimodal variability is not as clear as for winter because anomalies are generally weaker. Autumn variability looks like that of winter. Further work is needed to determine if signs of predictability for the winter season can be found in autumn.

This study strongly suggests further work. The cluster analysis and temperature impact methods could be applied to daily data, in order to link high-frequency weather variability with monthly to seasonal variability. This would allow us to determine if there exist some links between low-frequency climate regimes and their high-frequency counterparts, weather regimes. This may help to downscale seasonal forecasts to a weekly or daily time-scale, which would be more appropriate for numerous operational applications, such as energy demand forecasting and production management.

It would also be interesting to work on the time history of regime occurrence to detect if some transitions between two specific regimes are favoured. Succession of regimes could be studied with spectral analysis to underline oscillations (Simonnet and Plaut, 2001). Another important point would be to investigate lagged SST anomalies, both in ERA40 and DEMETER hindcasts, to determine if signs of predictability before winter can be found knowing the ocean state (Cassou et al., 2004b).

Finally, the DEMETER system is globally able to correctly simulate the winter monthly atmospheric variability in terms of pressure fields and temperature impacts. However, the predictability of regimes shows low scores. Nevertheless, it remains that reliable seasonal predictions from climate models would bring valuable information about winter climate regime forecasts on a monthly time-scale, as those regimes are clearly linked to specific impacts. Linking seasonal or monthly variability with weekly or daily variability, especially in terms of temperature anomalies, would be useful for electricity consumption forecast and production management in Europe.

7. Acknowledgments

We thank Laurent Terray (CERFACS) as we benefited from very fruitful discussions about climate regimes with him. We also thank the DEMETER team and especially Paco Doblas-Reyes, who helped us to obtain, understand and use the DEMETER seasonal forecast simulations.

References

Arkin, P. A. and Xie, P. 1994. The global precipitation climatology project: first algorithm intercomparison project. *Bull. Am. Meteorol. Soc.* **75**, 401–420.

Brier, G. W. 1950. Verification of forecasts expressed in terms of probability. *Mon. Wea. Rev.* **78**, 1–3.

Cassou, C., Terray, L., Hurrell, J. W. and Deser C. 2004a. North Atlantic winter climate regimes: spatial asymmetry, stationarity with time and oceanic forcing. *J. Climate* **17**, 1055–1068.

Cassou, C., Terray, L., Deser, C., Drévillon, M. and Hurrell, J. W. 2004b. Summer sea surface temperature conditions in the North Atlantic and their impacts upon the atmospheric circulation in early winter. *J. Climate* **17**, 3349–3363.

Delecluse, P. and Madec, G. 1999. Ocean modelling and the role of the ocean in the climate system. In: *Modeling the Earth's Climate and its Variability* (eds. W. R. Holland, S. Joussaume, and F. David), Elsevier Science, Amsterdam, 237–313.

Déqué, M. 2001. Seasonal predictability of tropical rainfall: probabilistic formulation and validation. *Tellus* **53A**, 500–512.

Diday, E. and Simon, J. C. 1976. Clustering analysis. In: *Communication and Cybernetics 10 Digital Pattern Recognition* (ed. K. S. Fu), Springer-Verlag, New York, 47–94.

Gordon, C., Cooper, C., Senior, C. A., Banks, H., Gregory, J. M. and co-authors. 2000. The simulation of SST, sea ice extents and ocean heat transports in a version of the Hadley Centre coupled model without flux adjustments. *Climate Dyn.* **16**, 147–168.

Gregory, D., Morcrette, J. J., Jakob, C., Beljaars, A. C. M. and Stockdale, T. 2000. Revision of convection, radiation and cloud schemes in the ECMWF Integrated Forecasting System. *Q. J. R. Meteorol. Soc.* **126**, 1685–1710.

Halpert, M. S. and Ropelewski, C. F. 1992. Surface temperature patterns associated with the Southern Oscillation. *J. Climate* **7**, 577–593.

Hurrell, J. W. 1995. Decadal trends in the North Atlantic Oscillation and relationships to regional temperature and precipitation. *Science* **269**, 676–679.

Hurrell, J. W., Kushnir, Y., Ottersen, G. and Visbeck, M. 2003. An overview of the North Atlantic Oscillation. In: *The North Atlantic Oscillation, Climatic Significance and Environmental Impact*, Geophysical Monograph Series 134, Washington, DC, 1–35.

Lorenz, E. N. 1963. Deterministic non-periodic flow. *J. Atmos. Sci.* **26**, 130–141.

Madec, G., Delecluse, P., Imbard, M. and Levy, C. 1997. *OPA Release 8, Ocean General Circulation Model Reference Manual*. LODYC Internal Report, Paris, 200 pp. (available from LODYC/IPSL, 4 Place Jussieu, 75252 Paris Cedex 05, France).

Madec, G., Delecluse, P., Imbard, M. and Levy, C. 1998. *OPA version 8.1 Ocean General Circulation Model Reference Manual*. LODYC Tech. Rep. 11, Paris, 91 pp. (available from LODYC/IPSL, 4 Place Jussieu, 75252 Paris Cedex 05, France).

Marsland, S. J., Haak, H., Jungclaus, J. H., Latif, M. and Röske, F. 2003. The Max-Planck-Institute global ocean/sea ice model with orthogonal curvilinear coordinates. *Ocean Modelling* **5**, 91–127.

Martineu, C. 1997. Contribution to climate seasonal forecasts evaluation. Analysis of winter atmospheric variability in Europe simulated by an AGCM. Thesis, Ecole Doctorale de Mécanique, Ecole Centrale De Lyon, Lyon, France (in French).

Martineu, C., Caneill, J. Y. and Sadourny, R. 1999. Potential predictability of european winters from the analysis of seasonal simulations with an AGCM. *J. Climate* **12**, 3033–3061.

Michelangeli, P.-A., Vautard, R. and Legras, B. 1995. Weather regimes: recurrence and quasi-stationarity. *J. Atmos. Sci.* **52**, 1237–1256.

Murphy, A. H. 1973. A new vector partition of the probability score. *J. Appl. Meteorol.* **12**, 595–600.

Palmer, T. N., Alessandri, A., Andersen, U., Cantelaube, P., Davey, M. and co-authors. 2004. Development of a European multi-model ensemble system for seasonal to interannual prediction (DEMETER). *Bull. Am. Meteorol. Soc.* **85**, 853–872.

Plaut, G. and Simonnet, E. 2001. Large-scale circulation classification weather regimes, and local climate over France, the Alps, and Western Europe. *Climate Res.* **17**, 303–324.

Pope, V. D., Gallani, M. L., Rowntree P. R. and Stratton, R. A. 2000. The impact of new physical parametrizations in the Hadley Centre climate model: HadAM3. *Climate Dyn.* **16**, 123–146.

Rodwell, M. J., Rowell, D. P. and Folland, C. K. 1999. Oceanic forcing of the wintertime North Atlantic Oscillation and European climate. *Nature* **398**, 320–323.

Roeckner, E. 1996. The Atmospheric General Circulation Model ECHAM-4: Model Description and Simulation of Present-Day Climate. Max-Planck-Institut für Meteorologie, Technical Report No 218, Hamburg, 90 pp. (available from Max-Planck-Institut für Meteorologie Bundesstr. 55, D-20146 Hamburg, Germany).

Sanders, R. A. 1953. Blocking highs over the Eastern North Atlantic and Western Europe. *Mon. Wea. Rev.* **81**, 67–73.

Simmons, A. J. and Gibson, J. K. 2000. *The ERA40 Project Plan*. ERA40 Project Report Series No. 1.

Simonnet, E. and Plaut, G. 2001. Space–time analysis of geopotential height and SLP, intraseasonal oscillations, weather regimes, and local climates over North Atlantic and Europe. *Climate Res.* **17**, 325–342.

Terray, L. and Cassou, C. 2002. Tropical Atlantic sea surface temperature forcing of quasi-decadal climate variability over the North Atlantic–European region. *J. Climate* **15**, 3170–3187.

Ulbrich, U. and Christoph, M. 1999. A shift of the NAO and increasing storm track activity over Europe due to anthropogenic greenhouse gas forcing. *Climate Dyn.* **15**, 551–559.

Vautard, R. 1990. Multiple weather regimes over the North Atlantic: analysis of precursors and successors. *Mon. Wea. Rev.* **118**, 2056–2081.

Ward, J. 1963. Hierarchical grouping to optimize an objective function. *J. Am. Stat. Assoc.* **58**, 236–244.

Wilks, D. S. 1995. Probability forecasts. In: *Statistical Methods in the Atmospheric Sciences*, Academic Press, New York, 258–272.

Wolff, J. E., Maier-Reimer, E. and Legutke, S. 1997. *The Hamburg Ocean Primitive Equation Model*. Deutsches Klimarechenzentrum Technical Report No. 13, Hamburg (available from Model and Data Group, c/o Max-Planck-Institut für Meteorologie Bundesstr. 55, D-20146 Hamburg, Germany).